0013-7227/01/$03.00/0
Printed in U.S.A.

The Journal of Clinical Endocrinology & Metabolism 86(8):3675–3685

Characterization of Human FSH Isoforms Reveals a Nonglycosylated β-Subunit in Addition to the Conventional Glycosylated β-Subunit

WENDY J. WALTON*, VAN T. NGUYEN, VLADIMIR Y. BUTNEV, VINOD SINGH, WILLIAM T. MOORE, AND GEORGE R. BOUSFIELD

Department of Biological Sciences, Wichita State University, Wichita, Kansas 67260-0026; Institute of Self-Organizing Systems and Biophysics, North-Eastern Hill University (V.S.), Shillong 793022, India; and Protein Chemistry Laboratory, University of Pennsylvania School of Medicine (W.T.M.), Philadelphia, Pennsylvania 19104

Human FSH consists of a mixture of isoforms that can be separated on the basis of differences in negative charge conferred by variations in the numbers of sialic acid residues that terminate oligosaccharide branches. Western analysis of human FSH isoforms separated by chromatofocusing revealed the presence of two human FSHβ isoforms that differed in size. A low mol wt human FSHβ isoform was associated with all FSH isoform fractions. A high mol wt human FSHβ isoform was associated with the more acidic fractions and increased in relative abundance as the pI decreased. Characterization of representative human FSHβ isoforms by mass spectrometry and automated Edman degradation revealed a low mol wt isoform that was not glycosylated. A high mol wt isoform was *N*-glycosylated at Asn residues 7 and 24. These results indicate that pituitary human FSH consists of two classes of molecules: those that possess a nonglycosylated β-subunit and those that possess a glycosylated β-subunit. Glycoprotein hormones are known to be elliptical molecules, and the β-subunit oligosaccharides project outward from the short diameter, thereby increasing it. It is interesting to speculate that this change in shape might affect ultrafiltration rates, leading to differences in delivery rates to target tissues and elimination by filtration in the kidney. (*J Clin Endocrinol Metab* 86: 3675–3685, 2001)

FSH IS KNOWN to exist as a dynamic population of isoforms that exhibit changes in relative abundance reflecting the endocrine status of the individual or the stage of the female reproductive cycle (1–4). An early report of FSH heterogeneity demonstrated the presence of two overlapping FSH isoforms in rhesus monkey pituitaries by Sephadex G-100 gel filtration (5). In intact females, the high mol wt form represented 37% of the total FSH immunoactivity, with the low mol wt form constituting the remainder. Ovariectomy produced an increase in the abundance of the high mol wt form to 58%. Elimination of *N*-glycosylation sites by site-directed mutagenesis has been shown to alter the Sephadex G-75 elution volumes for recombinant human FSHβ (hFSHβ) glycosylation mutants (6). Studies of FSH obtained from intact and gonadectomized rats and monkeys indicated that steroid hormones regulated size variation in this hormone (7–9). Application of high resolution electrophoretic and chromatographic techniques revealed the existence of multiple FSH isoforms in a variety of species, including our own (2). The biological activities of the isoforms varied, with the less acidic forms more active in various *in vitro* bioassays than the more acidic isoforms. Changes in isoform abundance were observed during the menstrual cycle (10). Removal of sialic acid from FSH oligosaccharides by neuraminidase digestion demonstrated that charge variation was largely due to differences in the sialic acid content of the different isoforms (11). Estradiol has been reported to reduce levels of sialyl transferase mRNA in rat pituitaries, which may contribute to the increase in less acidic FSH isoform abundance associated with elevated circulating levels of this hormone (12). Analysis of highly purified hFSH isoform preparations revealed that the sialic acid content ranged from 1.5 mol/mol hFSH in a less acidic isoform to 13.7 mol/mol in a more acidic isoform (13). Oligosaccharides isolated from hFSH differed primarily in the number of branches, which for the most part were terminated with sialic acid (14, 15). These were distributed across four *N*-glycosylation sites, two in the α-subunit and two in the β-subunit (16).

We became interested in characterizing the changing patterns of hFSH glycosylation at individual glycosylation sites when our studies with equine gonadotropin hybrids indicated equine FSH (eFSH) binding to its cognate receptor was less affected by αAsn^{56} oligosaccharide size than eLH (17). Taking the sialic acid content as an indicator of oligosaccharide branching, it seemed that hFSH isoforms could be isolated that possessed αAsn^{52} oligosaccharides with three or more branches for our studies. Our plan was to isolate a representative sample of hFSH isoforms from a human pituitary glycoprotein extract, separate the isoforms by means of chromatofocusing, and characterize the glycosylation of each isoform using techniques that are routine in our laboratory (18). We expected that oligosaccharide mapping would reveal a greater abundance of branched oligosaccharides in the more acidic hFSH isoforms. Instead, we encountered a nonglycosylated hFSHβ isoform. Because of the potential physiological significance of this isoform (19), our studies focused on characterizing it instead of counting oligosaccharide branches.

Abbreviations: CM, Carboxymethyl; eFSH, equine FSH; hFSH, human FSH; IRMA, immunoradiometric assay; MAb, monoclonal antibody; PBE-94, PolyBufferExchanger-94; WBB, Western blotting buffer.

Materials and Methods

Materials

Dr. Anne Hartree provided the human pituitary glycoprotein fraction, GTN, to Dr. Darrell N. Ward when she retired. Dr. Ward provided us with this fraction upon his retirement. The monoclonal antibody 46.3H6.B7 (20) was provided by Dr. James A. Dias (Wadsworth Center, New York State Department of Health, Albany, NY). Monoclonal antibodies RFSH20 (21), HT13 (22), and ECG01 (23) were provided by Dr. Jean-Michel Bidart (Insitut Gustave-Roussy, Villejuif, France). The monoclonal antibody 518B7 was provided by Dr. Janet Roser (University of California, Davis, CA) (24). The rabbit polyclonal antibody to eLHβ was prepared in this laboratory (25). The hLH and hFSH reference preparations were provided by the NIDDK National Hormone and Pituitary Program and Dr. A. F. Parlow. Dr. Gordon D. Niswender (Colorado State University, Bolder, CO) provided the antiserum against progesterone. Charcoal was purchased from EM Science (Gibbstown, NJ). Antimouse IgG or antirabbit IgG conjugated with horseradish peroxidase, amino acid standards, plus general and mammalian protease inhibitor cocktails were purchased from Sigma (St. Louis, MO). Tritiated progesterone was purchased from Amersham Pharmacia Biotech (Arlington Heights, IL). Dextran T500, ECL Western blotting detection reagent, carboxymethyl (CM)-Sephadex C-50, phenyl-Sepharose 6 fast flow, Sephacryl S-100, Sephadex G-75, and PolyBufferExchanger-94 (PBE-94) resins as well as Polybuffer 74 were obtained from Amersham Pharmacia Biotech (Piscataway, NJ). The semimicro pH electrode was purchased from Corning, Inc. (Big Flats, NY). Polyvinylidene difluoride Immobilon-P membranes and Amicon Centricon ultrafiltration chambers were obtained from Millipore Corp. (Bedford, MA). Prestained Broad Range Precision Protein Standard markers were purchased from Bio-Rad Laboratories, Inc. (Richmond, CA). Gel-code Blue stain was purchased from Pierce Chemical Co. (Rockford, IL). Scintisafe and Kodak Biomax ML Scientific Imaging Film were purchased from Fisher Scientific (St. Louis, MO). Medium 199, chicken serum, gentamicin, calf serum, and Benchmark Prestained Protein Ladder were obtained from Life Technologies, Inc. (Gaithersburg, MD). The plastic beads used in the immunoradiometric assay (IRMA) were purchased from Precision Plastic Ball Co. (Chicago, IL). The IRMAs were performed in 60-well plates obtained from Abbott Laboratories (Abbott Park, IL). All other reagents were sequencing grade, HPLC grade, or reagent grade as required.

The monoclonal antibody 46.3H6.B7 was raised against hFSH (20). It binds free FSHβ or FSH dimer, but does not cross-react with either α-subunit or hLHβ (26). Monoclonal antibody, RFSH20, was raised against recombinant hFSH (21). It binds hFSH and hFSHβ, but does not bind hLH, hCG, or α-subunit. It does exhibit a low level of binding to hTSH. Monoclonal antibody HT13 was raised against hCG (22) and recognizes an epitope spanning loops 1 and 3 that is specific to human α-subunits (22, 23). It can bind all human glycoprotein hormones via the common α-subunit. The monoclonal antibody, ECG01, was raised against eCG (27). It recognizes a conformational epitope in equine and human α-subunit loops 1 and 3 either as the isolated subunit or as part of a heterodimer (23). Bovine LH was used to prepare the monoclonal antibody 518B7, which binds free CG/LHβ and CG/LH dimer at a conformation-dependent epitope located on the β-subunit (24, 28). The polyclonal antibody, anti-eLHβ, was raised against eLHβ (29). This antibody recognizes denatured human and equine LH β-subunits when employed in Western blots and also recognizes denatured equine α-subunit (due to the 1.3% intact eLH content of the immunogen), but not human α-subunit.

Purification of hFSH

A 1.2-g batch of GTN was dissolved in 200 ml 4 mM ammonium acetate buffer, pH 5.7, at 4 C. Cation exchange chromatography using a 2.5 × 60-cm CM-Sephadex column, equilibrated in the same buffer, proceeded as described by Hartree (30), except that CM-Sephadex (C50) was substituted for CM-cellulose. The CM-Sephadex-bound fractions were subjected to phenyl-Sepharose chromatography. Samples ranging from 44–268 mg protein were dissolved in 1 M ammonium sulfate in 0.05 M sodium phosphate, pH 7.0, and applied to 2.5 × 13.2-cm columns of Amersham Pharmacia Biotech fast flow phenyl-Sepharose. The chromatograms were developed by stepwise elution as described by Hiyama *et al.* (31) at a flow rate of 270 ml/h. The FSH fractions obtained from three phenyl-Sepharose chromatograms were pooled and applied to a 2.5 × 190-cm column of Sephacryl S-100 that was equilibrated and developed with 0.126 M ammonium bicarbonate at a flow rate of 75 ml/h.

Separation of hFSH isoforms by chromatofocusing

Polybuffer 74 (PB-74) was diluted 1:8 with distilled water, and the pH was adjusted to 4.0 with HCl. A 0.9 × 40-cm PBE-94 column was equilibrated with 25 mM imidazole-HCl, pH 7.4, and developed with PB-74-HCl, pH 4.0, at a flow rate of 15 ml/h (32). The 46-mg hFSH sample was dissolved in PB-74 and equilibrated by gel filtration chromatography using a 2.5 × 33-cm Sephadex G-25 column equilibrated and developed with PB-74. The PBE-94 chromatogram was developed with PB-74, pH 4.0, at a flow rate of 16 ml/h. After the chromatogram returned to baseline during PB-74 elution, 1 M sodium chloride was applied to the column to elute the remaining bound protein. Protein peaks were detected by UV absorbance at 280 nm. The pH of each tube was measured using a semimicro pH electrode. A 0.3-ml aliquot of 1.1 M Tris-HCl, pH 7, was added to all fractions with a pH of 6 or less. Tubes were initially pooled into 16 different fractions, concentrated by lyophilization or by ultrafiltration using 10,000 mol wt cut-off Amicon Centriprep cartridges. Each fraction was then applied to a 2.5 × 94-cm Sephadex G-75 column that was equilibrated and developed with 0.126 M ammonium bicarbonate at a flow rate of 36 ml/h. Proteins detected by absorbance at 280 nm were recovered by lyophilization.

Immunoaffinity chromatography

Samples of the two most basic isoforms, 4.7 mg Cf-A and 1.0 mg Cf-B, were subjected to immunoaffinity chromatography at 4 C. One of the hFSH subunit fractions, Cf-C4, was also purified by immunoaffinity chromatography at 25 C. The hFSHβ-specific monoclonal antibody, 46.3H6.B7, was purified by protein G affinity chromatography, and the IgG fraction was coupled to a 1-ml Amersham Pharmacia Biotech Hi-Trap-NHS column following the instructions provided by the manufacturer. FSH or FSH subunit samples were diluted in 20 mM sodium phosphate buffer, pH 7.0. During initial experiments this buffer did not include protease inhibitors, whereas in subsequent experiments 1 mg/ml general protease inhibitors were included. The samples were vortexed, incubated for 15 min at 25 C, applied to the affinity column, and slowly recycled through the column for 30 min. The unbound material was eluted with 20 mM sodium phosphate, pH 7.0, and detected by absorbance at 280 nm using an in-line Uvicord II detector (Amersham Pharmacia Biotech). After the recorder pen returned to baseline, the bound fraction was eluted with 100 mM glycine-HCl, pH 2.7, and immediately neutralized by the addition of 180 μl/ml 1 M Tris-HCl, pH 9.0. Fractions were concentrated and desalted in Centricon P10 or Centriplus ultrafiltration devices and analyzed by Western analysis using RFSH20, HT13, and anti-eLHβ as described below. Amino acid analysis was performed on all four purified isoforms.

Subunit isolation

Two hFSH isoform samples, 2.9 mg Cf-C and 1.8 mg Cf-D, were incubated in 6 M guanidine hydrochloride at 37 C overnight with shaking. Each sample was then applied to a Phenomenex Jupiter C_{18} reverse phase HPLC column equilibrated with 80% 0.1 M sodium phosphate-triethylamine/20% 20 mM sodium phosphate-triethylamine, pH 6.5, containing 60% acetonitrile at a flow rate of 1 ml/min using a model 600 high performance liquid chromatograph (Waters Corp., Milford, MA). The column was washed for 10 min, then a 60-min linear gradient from 20–40% phosphate-triethylamine/acetonitrile was applied to elute the hFSH subunit fractions (31). Protein was detected by simultaneous measurement of absorbance at 280 and 210 nm using a model 490E detector (Waters Corp.). Proteins were desalted and concentrated using Amicon Centricon P10 devices. Fractions were analyzed by SDS-PAGE and Western analysis under reducing and nonreducing conditions with HT13 and RFSH20 antibodies. One fraction was subjected to immunoaffinity chromatography as described above. Samples of interest were subjected to amino acid analysis, mass spectrometry analysis, protein sequence analysis, and anti-eLHβ Western analysis.

SDS-PAGE

SDS-PAGE was routinely conducted using a Mini-PROTEAN II electrophoresis apparatus (Bio-Rad Laboratories, Inc., Richmond, CA). Samples were subjected to electrophoresis on 15% polyacrylamide slab gels, using the discontinuous buffer system of Laemmli (33) at a constant voltage of 200 V. Gels were fixed for at least 30 min in 9% acetic acid/45% methanol/46% water, stained with Gel-code Blue for at least 1 h, then destained in distilled water. Gel images were captured using a Gel Doc 1000 (Bio-Rad Laboratories, Inc.), and M_r estimates were made using the software package Quantity One (Bio-Rad Laboratories, Inc.).

Western blotting

Western blotting on Millipore Corp. Immobilon-P polyvinylidene difluoride membranes was performed as recommended by the manufacturer. Following SDS-PAGE, proteins were transferred to Immobilon-P membranes at 4 C for 2 h using a constant voltage of 100 V in a Mini-PROTEAN II transfer apparatus. The transfer buffer was composed of 25 mM Tris-HCl (pH 7.4), 190 mM glycine, and 20% methanol. After electroblotting, the membranes were blocked with 50 ml 5% (wt/vol) nonfat dry milk suspended in Western blotting buffer (WBB) composed of 150 mM sodium chloride, 1 mM EDTA, 50 mM Tris-HCl, and 0.05% Tween 20. After 1 h, the membranes were washed with distilled water followed by three 100-ml washes in WBB for 5 min each. Membranes were next incubated with one of the following protein G-purified monoclonal antibodies (MAb) RFSH20, HT13 (diluted 1:1000), or protein G-purified polyclonal anti-eLHβ antibody (5 μg) in 5 ml WBB containing 5% nonfat dry milk for 3–4 h. Membranes were washed three times in WBB. Secondary antibodies (5 μl) conjugated to horseradish peroxidase that were specific for mouse (RFSH20 and HT13) or rabbit (anti-eLHβ) IgG were added to 10 ml 5% milk in WBB, incubated with a membrane for 1 h, and then washed as described above. Finally, membranes were treated with Amersham Pharmacia Biotech enhanced chemiluminescence Western blotting detection reagents following the manufacturer's instructions. Blots were then exposed to Biomax ML Scientific Imaging Film for various times and processed with a film processor. Either Life Technologies, Inc., Benchmark Prestained protein ladder or Bio-Rad Laboratories, Inc., Prestained Broad Range Precision Protein Standards were used to estimate the sizes of the immunoreactive protein bands. X-Ray film images were captured using a Gel Doc 1000 (Bio-Rad Laboratories, Inc.). M_r estimation and volume analysis were carried out using the software package Quantity One. Volume analysis is densitometric analysis of a rectangular region of the SDS gel or x-ray film used in a Western blot.

Mass and sequence analysis

Matrix-assisted laser desorption ionization, time of flight mass spectrometry (34) was performed on a Micromass TofSpec 2E time of flight mass spectrometer (1.0-m flight tube) outfitted with a N2 UV laser (337 nm). Samples of purified hFSHα and hFSHβ isoform preparations were dissolved in 50% acetonitrile/0.1% trifluoroacetic acid and diluted before analysis using α-cyano-4-hydroxycinnamic acid as the matrix (35). Samples of the hFSHβ preparations were subjected to 24 cycles of automated Edman degradation using a PE Applied Biosystems (Foster City, CA) model 473A protein sequencer. Potential signal peptidase cleavage sites were investigated following the method of von Heijne (36) as implemented by the Macintosh software package AnalyzeSignalase version 2.03, written by Ned Mantei (Department of Biochemistry, Swiss Federal Institute of Technology, Zurich, Switzerland).

IRMAs

IRMAs (37) involved combinations of the common α-specific MAb HT13 or ECG01 with either the FSHβ-specific MAb RFSH20, or the LHβ-specific MAb 518B7. Tracer antibodies were diluted to 100,000 cpm/200 μl. Cold hormone and tracer dilutions were prepared in a solution of 50% 0.1 M sodium phosphate, pH 7.4, and 50% decomplemented calf serum. For each cold hormone dilution, two beads were incubated with capture antibodies at 25 C for 13 h with slow shaking. Beads were incubated with capture antibody HT13 to assess hLH contamination or with RFSH20 to measure hFSH. After incubation, the beads were washed with Milli-Q water three times and transferred to 60-well plates containing 100 μl cold hormone dilutions and 100 μl 50% 0.1 M sodium phosphate, pH 7.4, and 50% decomplemented calf serum. The plates were incubated at 25 C for 2 h with slow shaking. Blank control wells with buffer and tracer but no cold hormone served to measure background counts per min. After incubation, free hormone was aspirated from wells, and the beads were subsequently washed three times with Milli-Q water. After washing the beads, 200 μl tracer were added to each well. The tracer antibodies used were [^{125}I]518B7 for measuring hLH and [^{125}I]HT13 or [^{125}I]ECG01 for measuring hFSH. Tracer antibodies were incubated with the bead-hormone complex for 1 h at 25 C. After incubation, the supernatant was aspirated, and the beads were washed three times with Milli-Q water, transferred to polypropylene tubes, and counted in a Packard Cobra II AutoGamma counter. The counting efficiency was more than 74%. Statistical analysis of the families of dose-response curves was accomplished using the software package Allfit (38).

Radioligand assays

The LH RLA employed [^{125}I]hCG as radioligand and rat testis homogenate as LH receptor preparation (29). The specific activities ranged from 12–19 μCi/μg, and specific binding was 12–19% of the total counts added. The hLH standards employed were AFP-4179C (2162 IU/mg) and NIDDK/National Hormone and Pituitary Program AFP-4395A (6100 IU/mg). The FSH radioligand assay employed Chinese hamster ovary cells stably transfected with a human FSH receptor cDNA as the receptor preparation and [^{125}I]eFSH as radioligand (17). The specific binding of this tracer ranged from 15–36% of the total counts added. The hFSH reference preparation was NIDDK/National Hormone and Pituitary Program AFP-7298A SIAFP-B-3, which has a FSH potency of 8560 IU/mg. The program Allfit (38) was used to compare the dose-response curves and calculate relative potencies.

Granulosa cell assay

To compare the *in vitro* biological activities of the purified hFSH isoforms, progesterone secretion by diethylstilbestrol-primed granulosa cells obtained from immature female rats was measured in response to increasing concentrations of hormone preparation (17, 39). The progesterone content of 100-μl samples of conditioned medium was determined by RIA (40). The ED_{50} for each dose-response curve was determined using Allfit (38), and relative potency calculations were based on comparison of these values.

Results

Purification of hFSH

The isolation procedure consisted of chromatographic steps designed to minimize separation of the various hFSH isoforms. Indeed, the bulk of the FSH activity was associated with a single fraction recovered from the CM-Sephadex column and each phenyl-Sepharose column. After gel filtration of the combined hFSH fractions, we recovered 49 mg purified hFSH in Sephacryl S-100 fraction B that exhibited an FSH receptor binding potency of 2925 IU/mg. This represented 25% of the FSH activity in the GTN fraction. Comparison of the SDS-PAGE profiles for the hFSH preparations revealed more contaminant protein bands in S100-B than in AFP7298A (Fig. 1A). The electrophoretic mobilities of the two major bands associated with S100-B were greater than that of the major band associated with AFP7298A. The former resembled those of purified hLH, suggesting possible contamination. However, a receptor binding assay indicated only 4% LH receptor-binding activity associated with S100-B, and the results of an IRMA indicated only 2% LH immunoactivity. Western analysis of GTN, S100-B, and human gonadotropin reference preparations with an hFSHβ-specific monoclonal

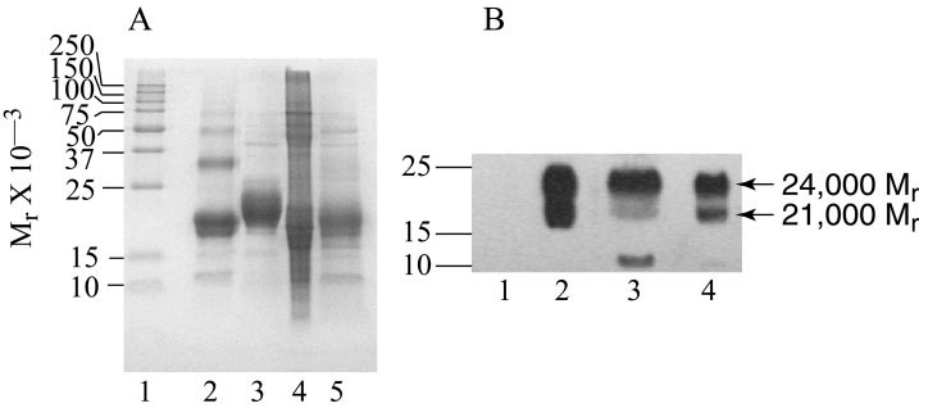

FIG. 1. Characterization of purified hFSH by SDS-PAGE and Western blotting. Hormone samples were electrophoresed on 15% polyacrylamide gels under reducing conditions. One gel was stained with Gel-code Blue. The other gel was electrotransferred to Immobilon-P, and the membrane was probed with an hFSHβ-specific monoclonal antibody RFSH20. A, SDS-PAGE. Lane 1, Bio-Rad Laboratories, Inc., prestained mol wt markers, as indicated; lane 2, 10 μg hLH (AFP4179C); lane 3, 10 μg hFSH (AFP7298A); lane 4, 30 μg GTN; lane 5, 10 μg hFSH (S100-B). B, Western blot. Lane 1, 1 μg hLH; lane 2, 0.6 μg hFSH; lane 3, 60 μg GTN; lane 4, 2 μg hFSH (S100-B). The positions of the mol wt markers are indicated.

antibody revealed the presence of two bands in all FSH-containing fractions (Fig. 1B). The 24,000 mol wt hFSHβ isoform band was more abundant than the 21,000 mol wt isoform. Densitometric analysis of the x-ray film with Quantity One software indicated that the 21,000 mol wt band represented 14% of the immunoreactive material in GTN. Its relative abundance increased to 24% in S100-B. An 11,000 mol wt hFSHβ fragment band was observed in the GTN fraction, but not AFP7298A. This apparent fragment band appeared to be associated with an hFSHβ fraction that was partially eliminated from S100-B by gel filtration chromatography.

Separation of hFSH isoforms

The chromatofocusing chromatogram consisted of very broad, overlapping peaks (Fig. 2A). Western analysis of the individual fractions revealed that the 21,000 mol wt hFSHβ isoform was present in all chromatofocusing fractions that possessed detectable hFSHβ (Fig. 2B). The 24,000 mol wt isoform was present only in the more acidic fractions, those eluted below pH 5.5, and its relative abundance increased as the pI decreased. The α-subunit band intensity appeared to be related to the amount of hLHβ present (Fig. 2C). Although hLH was expected in basic fractions, the level of hLHβ contamination in many of these fractions was surprisingly high (Fig. 2D), as we had only detected a 2–4% LH in the S100-B fraction.

Dimer-specific IRMAs confirmed the high abundance of hLH in the less acidic fraction 2 (Cf-A). In fact, there was more LH immunoactivity in the Cf-A fraction than in the S100-B fraction from which it was derived (17,775 *vs.* 6,808 IU/mg, respectively). This suggested FSH interference with the LH immunoradiometric assay. Due to limited amounts of 518B7 available, we used HT13, the α-specific antibody, as the capture antibody and detected hLH with the LHβ-specific antibody [^{125}I]518B7. FSH also binds HT13, and this could have limited hLH binding, producing a reduced estimate of LH present in S100-B. Reduction of the FSH concentration after chromatofocusing may have been responsible for the nearly 3-fold increase in LH immunoactivity that accompanied chromatofocusing. Western analysis indicated that Cf-B (fractions 4–9) was also predominantly hLH, although there was not enough material to include in the IRMA. We used immunoaffinity chromatography to purify hFSH from both Cf-A and Cf-B. The antibody-bound fractions were designated Cf-A* and Cf-B*. These preparations along with Cf-C (fractions 10–13) and Cf-D (fraction 15) provided us with four highly purified hFSH isoforms. Cf-A* and Cf-B* possessed primarily the low mol wt hFSHβ isoform, whereas Cf-C and Cf-D possessed both hFSHβ isoforms (Fig. 3A). Western analysis indicated that we had succeeded in largely eliminating hLHβ immunoactivity (Fig. 3C), which could only be detected after prolonged exposure of the x-ray film. However, densitometric analysis indicated that the intensity of the α-subunit bands varied considerably, with 30% that of AFP7298A hFSH present in Cf-A*, 7% in Cf-B*, 100% in Cf-C, and 66% in Cf-D (Fig. 3B). In contrast, the hFSHβ immunoactivity possessed by these fractions was relatively uniform, representing 56–64% that of AFP7298A hFSH. As the same variations in α-subunit immunoactivity were obtained after probing three different Immobilon-P membranes with HT13, we suspected that Cf-A* and Cf-B* possessed more hFSHβ than hFSH. Indeed, a subsequent dimer-specific IRMA that used RFSH20 as capture antibody and ECG01 as tracer indicated that that Cf-B* possessed only 2% hFSH immunoactivity.

FSH receptor binding and steroidogenic potencies of hFSH isoforms

FSH radioligand assays of Cf-A*, Cf-C, and Cf-D (Fig. 4A) indicated the same level of FSH receptor-binding activity in these three fractions (mean potency $\pm$ SD, 3,548 $\pm$ 1,515, 1,791 $\pm$ 272, and 1,421 $\pm$ 352 IU/mg, respectively). This suggested that despite the reduced α-subunit immunological activity observed in Cf-A*, it was primarily an hFSH dimer preparation. When the FSH activities were compared in the more sensitive granulosa cell assay that permitted inclusion of Cf-B* (Fig. 4B), this preparation exhibited only 5% FSH biological activity (457 IU/mg). It possessed 8 times more

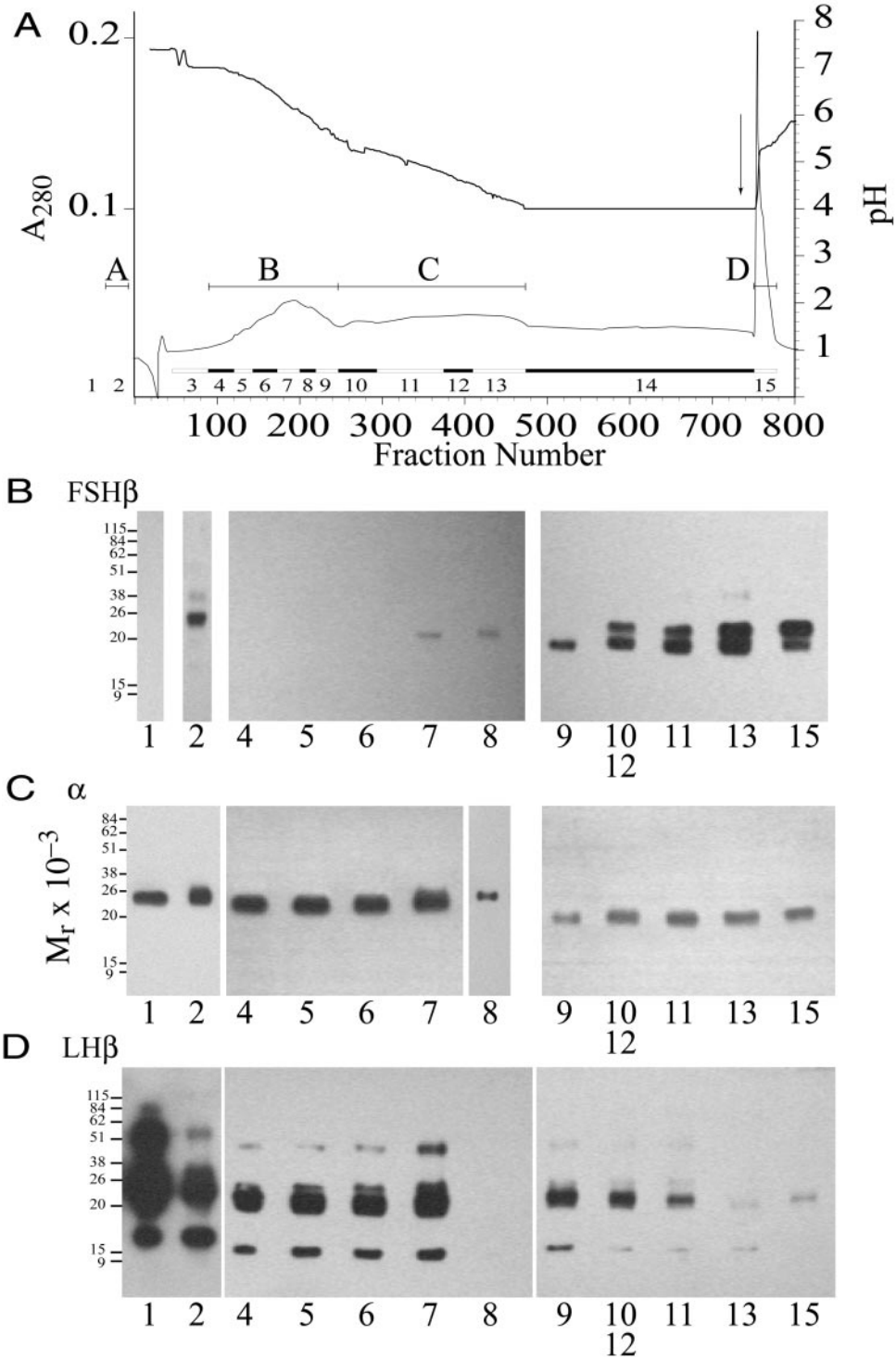

FIG. 2. Separation of hFSH isoforms by chromatofocusing. A, Separation of a 46-mg sample of the purified hFSH preparation, S100-B on a PBE-94 column using a pH 7 to pH 4 gradient, as indicated. The column went dry during sample application; therefore, the unabsorbed fractions were recovered from the washes used to remove the dried resin from the column. These are indicated by the numbers 1 and 2 outside the chromatogram. The alternating *open* and *closed bars* indicate the fractions combined and chromatographed over Sephadex G-75. Fractions containing protein were analyzed by Western blotting after SDS-PAGE of 2-μg samples under reducing conditions. Based on the results of experiments shown in B and C, the initial column fractions were pooled, as indicated by *brackets*. Because it was not possible to fit all of the samples on one blot, each panel shows a collage of individual membranes. B, Western analysis using the FSHβ-specific monoclonal antibody RFSH20. C, Western analysis using the human α-subunit-specific monoclonal antibody HT13. D, Western analysis using LHβ-specific polyclonal antibody, anti-eLHβ. The numbers *below* each panel correspond to the fractions indicated in A.

hFSHβ immunoactivity than α-subunit immunoactivity as indicated by Western analysis and 2% hFSH by IRMA, consistent with the presence of more biologically inactive hFSHβ than functional hFSH heterodimer. Although the Cf-A* FSH receptor-binding activity was not significantly greater than that of Cf-C and Cf-D ($P > 0.05$), its FSH potency in the granulosa cell assay increased 4-fold, giving Cf-A* a greater FSH activity (14,545 IU/mg) than the hFSH reference preparation AFP7298A. Cf-C and Cf-D had FSH potencies of 1,238 and 1,615 IU/mg, respectively. Unfortunately, there was not enough material to further characterize Cf-A*.

Subunit isolation and characterization

The more abundant hFSH isoform preparations, Cf-C and Cf-D, were used for subunit purification. The former pos-

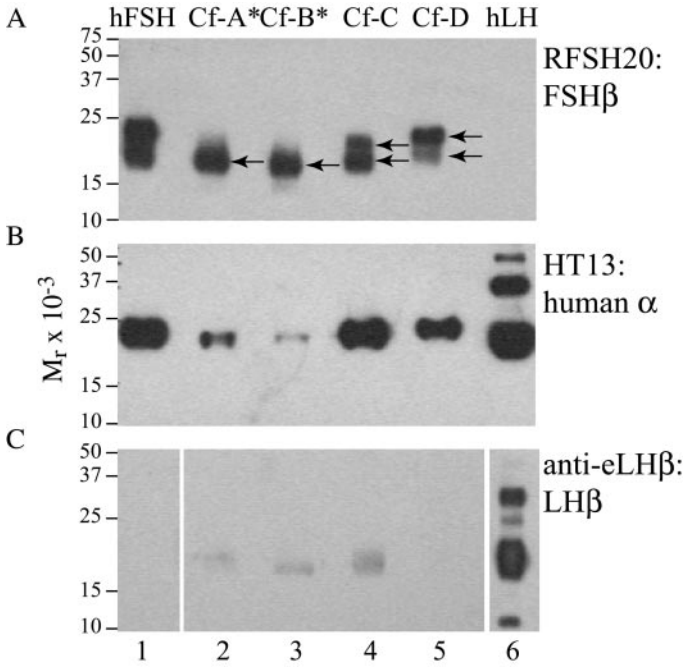

FIG. 3. Western blot analysis of purified hFSH isoforms. Three sets of purified hFSH isoform preparation samples were subjected to SDS-PAGE under reducing conditions, transferred to Immobilon-P, and probed with FSHβ-, α-subunit-, and LHβ-specific antibodies as indicated. A, FSHβ-specific Western blot employing MAb RFSH20 after a 35-sec exposure. The *arrows* indicate the 21,000 and 24,000 mol wt hFSHβ isoform bands. B, Human α-subunit-specific Western blot with MAb HT13 after a 20-min exposure. C, LHβ-specific Western using a polyclonal antibody raised against eLHβ that recognized only hLHβ. The results after a 20-min exposure represent a single blot; however, the lane corresponding to hLH was cut out and moved to the same position as in A and B. Sample loads for hFSH preparations were based on amino acid analysis. The hLH value represents the weight of lyophilized protein that was analyzed. Lane 1, 0.1 μg hFSH (AFP7298A); lane 2, 0.1 μg Cf-A*; lane 3, 0.1 μg Cf-B*; lane 4, 0.1 μg Cf-C; lane 5, 0.1 μg Cf-D; lane 6, 0.8 μg hLH (AFP0642B).

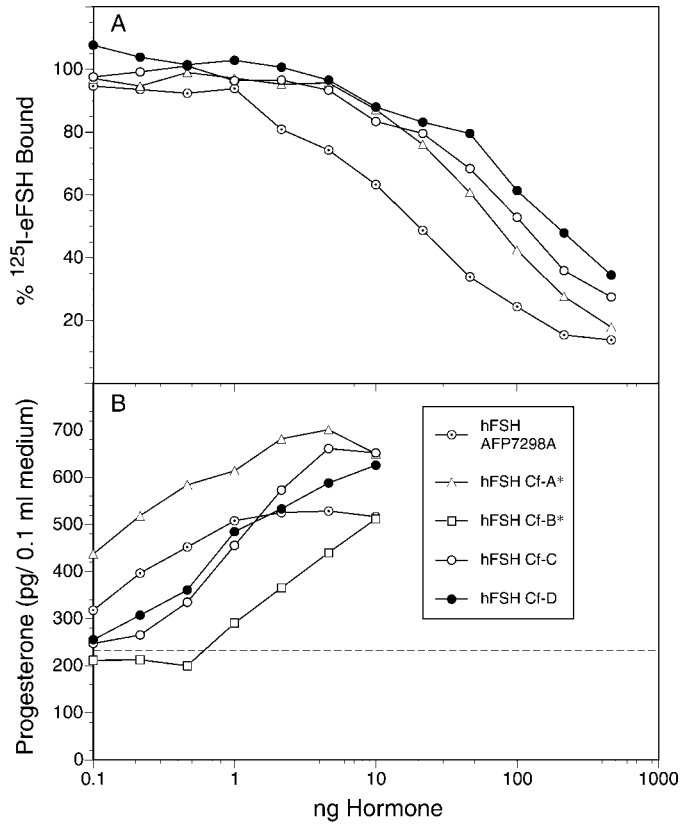

FIG. 4. FSH biological activities of hFSH isoforms. A, FSH receptor-binding activities of three of the four hFSH isoforms determined in a heterologous radioligand assay (there was insufficient Cf-B* to include in the assay). The tracer was [^{125}I]eFSH, and the receptor preparation consisted of CHO cells expressing the human FSH receptor. B, Granulosa cell bioassay. The granulosa cells were harvested from female rat ovaries that had been stimulated with diethylstilbestrol for 6 d. Progesterone was measured in conditioned culture medium samples after 72-h incubation. Hormone doses were determined by amino acid analysis.

sessed less than 50% of the 24,000 mol wt hFSHβ isoform, whereas the latter possessed 77% of this isoform. The relative abundance of the 24,000 mol wt hFSHβ isoform was reflected in the HPLC chromatograms (Fig. 5). The Cf-D subunit chromatogram included a peak at 27 min that produced an electrophoretic pattern indicating that it was probably the 24,000 mol wt hFSHβ isoform (Fig. 5B, *inset*, lane 4). This was confirmed by Western analysis (Fig. 6C). The absence of hFSHα immunoactivity from Cf-D3 indicated that it was suitable for characterization of its glycosylation. Fractions Cf-D4 and Cf-D5 appeared to be hFSHα. Cf-D6 was probably hFSH, as both α- and β-subunits were present, whereas Cf-D7 was composed primarily of the 24,000 mol wt hFSHβ isoform. The results were different when we tried to isolate subunits from Cf-C. There was only a shoulder at 27 min that produced a much broader Coomassie blue-stained band than that associated with Cf-D3. Western analysis indicated that Cf-C2 included the 24,000 mol wt hFSHβ isoform along with hFSHα. In fact, all of the fractions recovered from this chromatogram included both subunits. Fraction Cf-C4 appeared to be the best candidate for isolating the 21,000 mol wt hFSHβ isoform. As Western analysis of nonreduced samples of this fraction indicated that it was predominantly dissociated subunit (data not shown), we purified the hFSHβ component by immunoaffinity chromatography using the same procedure employed to obtain Cf-A* and Cf-B*.

Analysis of hFSHβ isoform glycosylation

The mass of the major component in the low mol wt hFSHβ isoform preparation, Cf-C4 (Fig. 7A), was 12,361.3. This was 124.9 mass units less than the average isotopic mass of 12,486.2 predicted from the amino acid sequence of hFSHβ, whereas the minor component was 80.4 mass units larger. The mass of the major component in the high mol wt hFSHβ isoform preparation, Cf-D3 (Fig. 7B), was 13,450.0, which was 963.8 mass units larger than the average isotopic mass of the peptide moiety of hFSHβ, whereas the minor component was 127.3 mass units smaller. Only the high mol wt hFSHβ isoform represented by Cf-D3 appeared to be glycosylated, as at least five overlapping peaks could be discerned in the expanded mass spectrum (Fig. 7B, *inset*). The Edman sequencing results corroborated the absence of glycosylation in the low mol wt hFSHβ isoform Cf-C4 and revealed that the

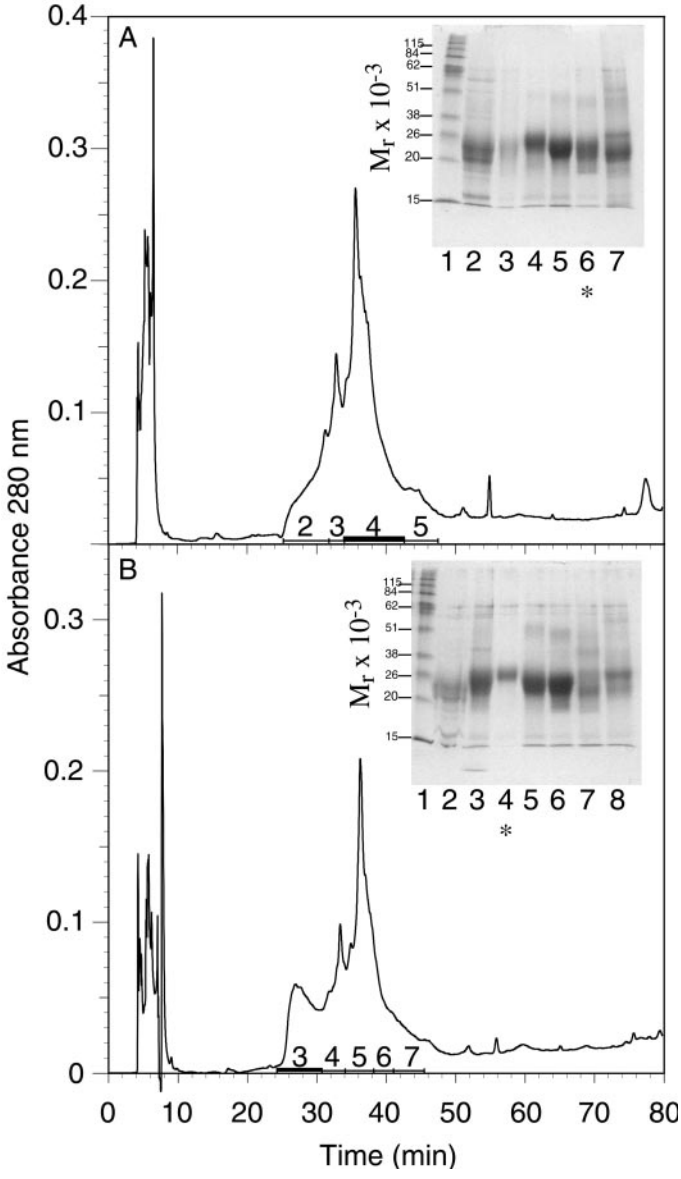

FIG. 5. FSH subunit isolation by reverse phase HPLC. FSH preparations were dissociated into subunits by incubation in 6 M GuHCl at 37 C overnight. Samples were subjected to reverse phase HPLC as described in *Materials and Methods*, and protein were recovered by evaporation in a Savant (Holbrook, NY) Speed-Vac. Portions of the chromatogram that were pooled to obtain the subunit preparations are indicated. SDS-PAGE was performed on 15% polyacrylamide gels under reducing conditions, followed by staining with Gel-code Blue. A, Subunit isolation from Cf-C. Gel *inset*: lane 1, mol wt markers; lane 2, 10 μg S100-B; lane 3, 10 μg Cf-C; lane 4, 10 μg Cf-C2; lane 5, 10 μg Cf-C3; lane 6, 10 μg Cf-C4; lane 7, 10 μg Cf-C5. B, Subunit isolation from Cf-D. Gel *inset*: lane 1, mol wt markers; lane 2, 10 μg S100-B; lane 3, 10 μg CF-D; lane 4, 10 μg Cf-D3; lane 5, 10 μg Cf-D4; lane 6, 10 μg Cf-D5; lane 7, 10 μg Cf-D6; lane 8, Cf-D7. The *asterisks* identify the lanes containing hFSHβ isoform fractions that were further characterized.

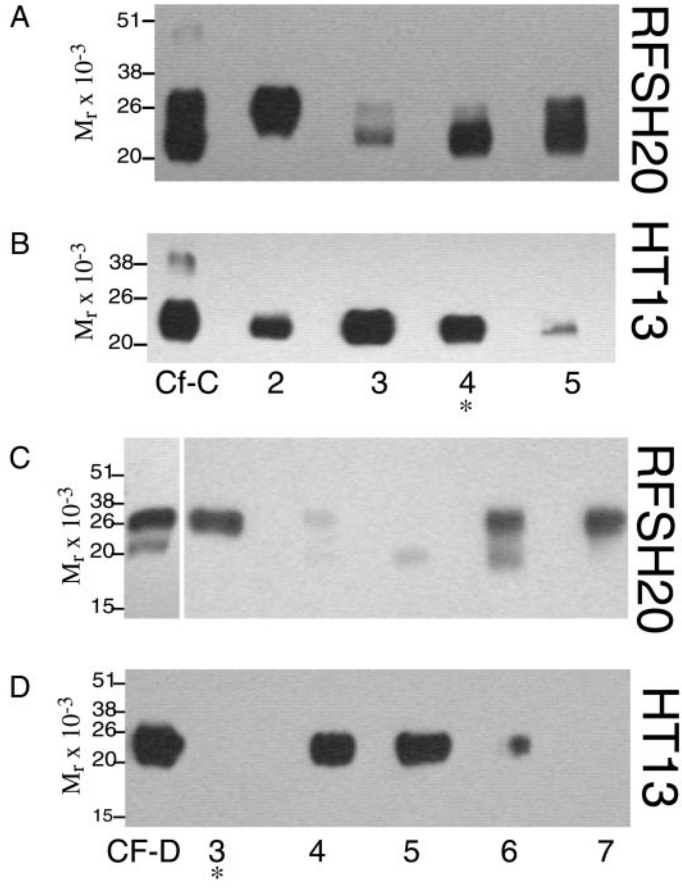

FIG. 6. Western analysis of FSH subunit fractions. Samples obtained from the chromatograms in Fig. 5 were subjected to SDS-PAGE under reducing conditions, transferred to Immobilon-P membranes, and probed with either FSHβ- or α-specific monoclonal antibodies, RFSH20 and HT13, respectively. Lanes are identified by the designation of the hFSH preparation or HPLC fraction. A and B, Western analysis of 2-μg samples of Cf-C subunit preparations, as indicated. C and D, Western analysis of 2-μg samples of Cf-D subunit preparations, as indicated. The *asterisks* identify the fractions used in subsequent analysis.

smaller than predicted mass for the main component was due to a two-residue deletion at the amino-terminus. A major sequence beginning with Cys^3 and a minor sequence beginning at Asn^1 were apparent in the >PhNCS-amino acid chromatograms. The 205.6-mass unit difference between the two components mass labeled 12,566.6 and 12,361.0 shown in Fig. 7A was very close to the 201.2-mass unit difference calculated from the hFSHβ 1–111 and 3–111 peptide sequences using the PeptIdent tool available at the SWISS-PROT/TrEMBL web site (41). Amino-terminal heterogeneity has been reported for FSH β-subunits derived from pituitary FSH (42–44). Until recombinant hFSHβ was analyzed, the heterogeneity was commonly attributed to postmortem degradation (45). However, the report that insect cell-expressed hFSHβ possessed an amino-terminal Cys^3 suggested this resulted from alternative signal peptidase cleavage (46). Analysis of the predicted sequence for pre-hFSHβ using the method of von Heijne (36) produced a lower score for cleavage at Cys^{-1}–Asn^1 (3.36) than for cleavage at Ser^2–Cys^3 (5.37). In contrast, similar scores (3.93 and 3.35, respectively) were obtained for pre-eFSHβ, which corresponded to the roughly equivalent amounts of the 1–111 and 3–111 forms found in this species (44). It was interesting that evidence for only the 3–111 hFSHβ form was obtained during automated Edman analysis of the

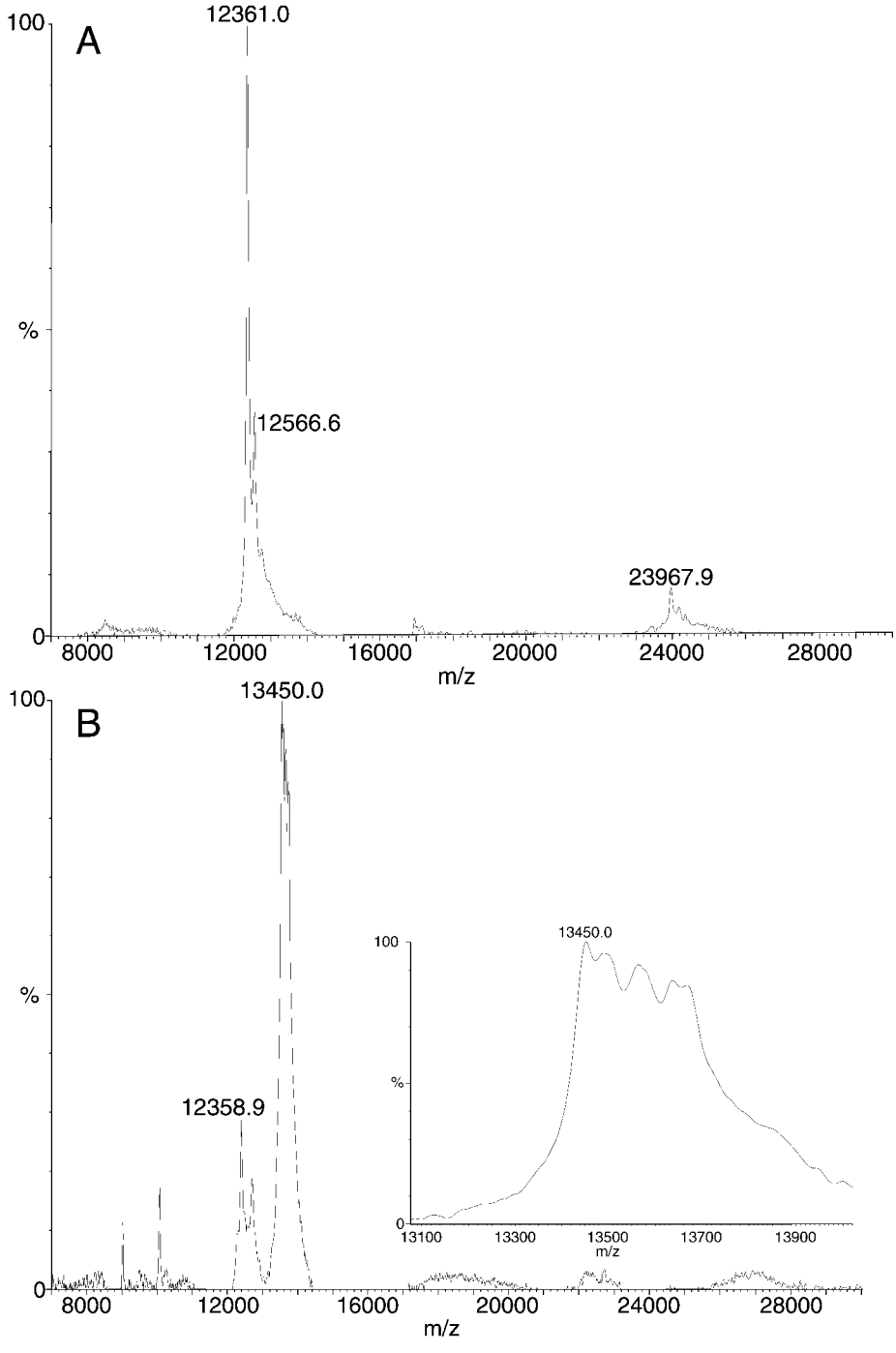

FIG. 7. Mass spectrometry of hFSHβ isoforms. Samples were analyzed by matrix-assisted laser desorption ionization, time of flight mass spectrometry using a Micromass TofSpec 2E time of flight mass spectrometer. A, Analysis of the 21,000 mol wt hFSHβ isoform Cf-C4. B, Analysis of the 24,000 mol wt hFSHβ isoform Cf-D3.

glycosylated hFSHβ isoform (see below), because both the 1–111 and 3–111 forms were associated with the diglycosylated and monoglycosylated eFSHβ isoforms (Bousfield, G. R., unpublished data), suggesting there is probably no relationship between signal peptidase cleavage and *N*-glycosylation. The fact that one signal peptidase cleavage site appeared to be favored over the other was crucial in permitting us to examine the glycosylation status of both hFSHβ *N*-linked sites. >PhNCS-Asn was observed during Edman degradation cycles corresponding to Asn^{7} and Asn^{24}, which indicated that some of the hFSHβ isoform contained in Cf-C4 had never been glycosylated. Amino acid sequence analysis of Cf-D3 indicated that it was also a truncated hFSHβ isoform consisting of residues 3–111. No >PhNCS-Asn was detected at either glycosylation site, indicating that the hFSHβ isoform CD-D3 was glycosylated at both Asn^{7} and Asn^{24}. Subtracting the mass predicted for hFSHβ 3–111 from the mass assigned to Cf-D3 yielded a combined mass of only 1,165 for the two oligosaccharides. This seemed small for the hFSHβ isolated from the most acidic hFSH isoform, especially since the most abundant hFSH oligosaccharides were reported to be

triantennary structures (15) with formula weights of 3,066. The presence of triantennary oligosaccharides predicted a mass of 18,700; however, no convincing signal was obtained in that region of the spectrum. In contrast, nonglycosylated hFSHβ 3–111 was observed even though its presence was undetectable by Western analysis (Fig. 6C).

Matrix-assisted laser desorption ionization, time of flight mass spectrometry analysis of hFSHα-subunits obtained from hFSH isoform preparations Cf-C3 and Cf-D5 yielded masses of 13,796.3 and 14,377.1, respectively. These peaks covered very broad ranges compared with the glycosylated hFSHβ isoform. The corresponding heterodimer masses ranged from 26,363 for the nonglycosylated hFSHβ isoform to 27,827 for the diglycosylated hFSHβ isoform. These were unexpectedly low because the electrophoretic mobilities of hFSH subunits were less than those for eFSH, indicating a greater mass for hFSH (47), yet the masses for the eFSH isoforms ranged from 28,199–31,059 (44).

Discussion

Partial glycosylation of FSH subunits was first reported for recombinant bFSHβ (48). Equine FSHβ was the first naturally occurring FSH subunit reported to exhibit partial glycosylation. This occurred at a single glycosylation site, Asn^7 (44). When we observed the two-band pattern after Western analysis of immunopurified hFSHβ, we anticipated that the 24,000 mol wt band represented the diglycosylated band, whereas the 21,000 mol wt band represented the monoglycosylated band. The existence of partially glycosylated FSHβ should have been observed during amino acid sequence determination; however, the low abundance of this isoform combined with subunit purification techniques that favored isolation of more heavily glycosylated FSHβ isoforms probably ensured that only the diglycosylated FSHβ isoform was obtained. Typically FSH subunits were separated by anion exchange chromatography (49–53). Nonglycosylated FSHβ probably was eluted in the unabsorbed fraction, whereas the absorbed fraction was enriched for the diglycosylated form. Even reverse phase HPLC, once touted as the universal solution to glycoprotein hormone subunit isolation (31, 54), was inadequate to separate the subunits derived from Cf-C in which the nonglycosylated β-subunit predominated. The chromatogram obtained during HPLC isolation of pFSH subunits indicated that porcine FSHβ was obtained from a peak that resembled the hFSHβ 27 min peak from which diglycosylated FSHβ was obtained in the present study (43).

The high biological potency of Cf-A* in the granulosa cell assay corresponded to results reported by Bishop *et al.* (55) for recombinant hFSH possessing a mutated, nonglycosylated hFSHβ expressed by CHO cells. Although elimination of both hFSHβ glycosylation sites had no effect on FSH receptor-binding activity, there was a 6-fold increase in FSH biological activity in the rat Sertoli cell bioassay. Recombinant hFSH expressed in COS-7 cells displayed increased FSH receptor-binding activity after hFSHβ glycosylation site deletion that was accompanied by decreased FSH biological activity in the rat granulosa cell bioassay (6). These contrasting results could be accounted for by differences in glycosylation resulting from expression in different cell types. However, no carbohydrate data were available, and other explanations, such as the use of RIA (55) *vs.* radioligand assay (6) to quantify the recombinant hFSH included in the assay, Sertoli cells *vs.* granulosa cells, proteolytic damage, or serum factor interference with the assays, made interpretation difficult. Our results contrast with those involving purified hFSH preparations, which suggested the less acidic hFSH isoforms were less active in RIAs and radioligand assays, whereas more acidic isoforms were more active (56). In the present study the least acidic preparation, Cf-A*, exhibited greater biological activity than the more acidic preparations, Cf-C and Cf-D. This result was consistent with studies involving crude hFSH isoform preparations; less acidic isoforms exhibited greater *in vitro* biological activity (2).

Based on β-subunit glycosylation, FSH could be divided into two categories: diglycosylated β-subunit, which possessed both *N*-linked oligosaccharides, and underglycosylated β-subunit. The latter appeared to take two forms. In horses, partially glycosylated eFSHβ lacked carbohydrate at Asn^7, but appeared to be glycosylated at Asn^{24}. In hFSHβ, it appeared that neither glycosylation site was occupied by carbohydrate. This was contrary to our expectation that a monoglycosylated hFSHβ isoform would be encountered. As recombinant hFSHβ includes an isoform lacking carbohydrate at Asn^{24} (26), the existence of a similar, naturally occurring hFSHβ isoform remains an open question. For the present discussion we will refer to the low mol wt hFSHβ isoform as a nonglycosylated isoform. All hFSH isoforms were found to possess hFSH with nonglycosylated hFSHβ as determined by characterization of representative high and low mol wt hFSHβ isoforms. More acidic hFSH isoforms possessed both the nonglycosylated and the diglycosylated hFSHβ isoforms. The relative abundance of the diglycosylated hFSHβ isoform increased with decreasing pI of the hFSH isoform. Nevertheless, even the most acidic hFSH isoforms possessed some of the nonglycosylated FSHβ isoform. Shorter circulatory half-lives have been reported for the less acidic FSH isoforms (57). Site-directed mutagenesis of recombinant hFSH indicated that the β-subunit oligosaccharides determined the MCRs (19). The present study demonstrates that the relative abundance of nonglycosylated hFSHβ is an additional factor contributing to the MCRs for various hFSH isoforms. Particularly relevant for our studies, a 5-fold increase in the MCR was observed after elimination of the Asn^7 glycosylation site and a 10-fold increase in clearance rate was noted after elimination of both glycosylation sites (19). Because less acidic hFSH isoforms possessed only the nonglycosylated β-subunit isoform, the more rapid clearance of these forms reflected this structural feature. The fact that a 10-fold difference in clearance rates has not been noted for naturally occurring hFSH isoforms probably reflected the heterogeneous nature of the more acidic isoform population, as both nonglycosylated and diglycosylated hFSHβ comprised the FSH molecules found in these isoform preparations.

Both hepatic and renal clearance mechanisms must be considered for glycoprotein hormones (4). Renal clearance may be more important for largely sialylated glycoprotein hormones, such as hFSH (58), as exclusively sialylated hCG

was not cleared by the liver asialoglycoprotein receptor (59). For proteins with masses less than 66,200, the mass of serum albumin, factors that determine glomerular ultrafiltration rate are size, shape, and charge (60). Carbohydrate can change all three factors, although the greatest effects are likely to be on molecular shape and charge. The crystal structure of hCG revealed an elongated molecule with molecular dimensions of 75 × 30 × 35 Å (61). The recent report of the crystal structure for hFSH confirmed the expectation that it has a similar elongated shape (26). Modeling of hCG oligosaccharides showed the two β-subunit oligosaccharides extending out from the narrow axis of the protein moiety (62). As this would increase the narrow diameter by as much as 30 Å (63), a substantial reduction in glomerular sieving could be expected. Indeed, reduced molecular size during gel filtration experiments has been demonstrated for recombinant hFSH mutants lacking one or more β-subunit glycosylation sites (6).

Less acidic FSH isoforms are elevated in the preovulatory phase of the reproductive cycle. Studies with deglycosylated ovine FSH indicated a more rapid uptake by the follicular granulosa cells (64). Perhaps partial or total elimination of FSHβ oligosaccharides is necessary for more efficient delivery to this avascular tissue, and the faster clearance rate is a by-product of a more rapid ultrafiltration rate necessary to facilitate ovarian uptake. Studies involving hFSH isoforms indicated that less acidic isoforms were more active in a bioassay that measured germinal vesicle breakdown in cumulus-enclosed mouse oocytes (65). Although recombinant hFSH mutants lacking both β-subunit glycosylation sites did not support increased ovarian weight gain in rats, there could be a specialized function for them. The cumulus-surrounded oocyte in a preovulatory follicle is located at the greatest distance from the vascularized theca cell layer. Less acidic FSH isoforms may be adapted to activating oocytes in preovulatory follicles because the absence of β-subunit oligosaccharides facilitates delivery to the interior of the follicle, increasing exit from follicle capillaries via ultrafiltration and more rapid diffusion through the interstitial fluid.

FSH glycosylation appears to be more complex than that of the other glycoprotein hormones. Partial glycosylation of the β-subunit must be considered along with the distribution of variably branched oligosaccharides (15, 58). Glycosylation mutants of the FSH β-subunit (6, 55) are now relevant subjects for studies on the physiological effects of FSH isoforms, but analysis of the impact of various oligosaccharide structures is rendered more difficult because FSH isoforms consist of mixtures of β-subunit isoforms.

Acknowledgments

We thank Drs. A. S. Hartree and D. N. Ward for providing the human glycoprotein hormone fraction that made these studies possible. We thank Drs. J.-M. Bidart, J. A. Dias, J. Roser, and G. D. Niswender for providing antibodies, and the NIDDK/National Hormone and Pituitary Program and Dr. A. F. Parlow for the hFSH and hLH reference preparations. We are grateful to Dr. Viktor Y. Butnev for his advice on chromatographic procedures.

Received November 22, 2000. Accepted March 30, 2001.

Address all correspondence and requests for reprints to: Dr. George R. Bousfield, Department of Biological Sciences, Box 26, Wichita State University, 1845 Fairmount, Wichita, Kansas 67260-0026. E-mail: george.bousfield@wichita.edu.

This work was supported by NIH Grant AG15428. Protein sequencing and mass spectrometry were provided by the Protein Chemistry Laboratory of the Medical School of the University of Pennsylvania supported by core grants of the Diabetes and Cancer Centers (DK-19525 and CA-16520).

* Present address: Program in Molecular Biophysics, Florida State University, Tallahassee, Florida 32306.

References

1. **Chappel SC, Ulloa-Aguirre A, Coutifaris C** 1983 Biosynthesis and secretion of follicle-stimulating hormone. Endocr Rev 4:179–211
2. **Ulloa-Aguirre A, Midgley Jr AR, Beitins IZ, Padmanbhan V** 1995 Follicle-stimulating isohormones: characterization and physiological relevance. Endocr Rev 16:765–787
3. **Ulloa-Aquirre A, Timossi C, Damian-Matsumura P, Dias JA** 1999 Role of glycosylation in function of follicle-stimulating hormone. Endocrine 11: 205–215
4. **Rose MP, Das REG, Balen AH** 2000 Definition and measurement of follicle stimulating hormone. Endocr Rev 21:5–22
5. **Peckham WD, Yamaji T, Dierschke DJ, Knobil E** 1973 Gonadal function and the biological and physicochemical properties of follicle stimulating hormone. Endocrinology 92:1660–1666
6. **Flack MR, Froehlich J, Bennet AP, Anasti J, Nisula BC** 1994 Site-directed mutagenesis defines the individual roles of the glycosylation sites on follicle-stimulating hormone. J Biol Chem 269:14015–14020
7. **Bogdanove EM, Campbell GT, Peckham WD** 1974 FSH pleomorphism in the rat–regulation by gonadal steroids. Endocr Res Commun 1:87–99
8. **Peckham WD, Knobil E** 1976 Qualitative changes in the pituitary gonadotropins of the male rhesus monkey following castration. Endocrinology 98: 1061–1064
9. **Peckham WD, Knobil E** 1976 The effects of ovariectomy, estrogen replacement, and neuraminidase treatment on the properties of the adenohypophysial glycoprotein hormones of the rhesus monkey. Endocrinology 98:1054–1060
10. **Zambrano E, Olivares A, Mendez JP, et al.** 1995 Dynamics of basal and gonadotropin-releasing hormone-releasable serum follicle-stimulating hormone charge isoform distribution throughout the human menstrual cycle. J Clin Endocrinol Metab 80:1647–1656
11. **Ulloa-Aguirre A, Miller C, Hyland L, Chappel S** 1984 Production of all follicle-stimulating hormone isohormones from a purified preparation by neuraminidase digestion. Biol Reprod 30:382–387
12. **Damian-Matsumura P, Zaga V, Maldonado A, Sanchez-Hernandez C, Timossi C, Ulloa-Aquirre A** 1999 Oestrogens regulate pituitary α2,3-sialyltransferase messenger ribonucleic acid levels in the female rat. J Mol Endocrinol 23:153–165
13. **Stanton PG, Shen Z, Kecorius EA, Bergon PG, Roberson DM, Hearn MT** 1995 Application of a sensitive HPLC-based fluorometric assay to determine the sialic acid content of human gonadotropin isoforms. J Biochem Biophys Methods 30:37–48
14. **Baenziger JU, Green ED** 1988 Pituitary glycoprotein hormone oligosaccharides: structure, synthesis and function of the asparagine-linked oligosaccharides on lutropin, follitropin and thyrotropin. Biochim Biophys Acta 947: 287–306
15. **Renwick AGC, Mizuochi T, Kochibe N, Kobata A** 1987 The asparagine-linked sugar chains of human follicle-stimulating hormone. J Biochem 101:1209–1221
16. **Moyle WR, Campbell RK** 1996 Gonadotropins. In: Adashi EY, Rock JA, Rosenwaks Z, eds. Reproductive endocrinology, surgery, and technology. Hagerstown: Lippincott-Raven; vol 1:683–724
17. **Butnev VY, Gotschall RR, Butnev VY, Baker VL, Moore WT, Bousfield GR** 1998 Hormone-specific inhibitory influence of α-subunit Asn^{56} oligosaccharide on *in vitro* subunit association and FSH receptor binding of equine gonadotropins. Biol Reprod 58:458–469
18. **Bousfield GR, Baker VL, Gotschall RR, Butnev VY, Butnev VY** 2000 Carbohydrate analysis of glycoprotein hormones. Methods 21:15–39
19. **Bishop LA, Nguyen TV, Schofield PR** 1995 Both of the β-subunit carbohydrate residues of follicle-stimulating hormone determine the metabolic clearance rate and *in vivo* potency. Endocrinology 136:2635–2640
20. **Weiner RS, Dias JA, Andersen TT** 1991 Epitope mapping of human follicle stimulating hormone-α using monoclonal antibody 3A identifies a potential receptor binding sequence. Endocrinology 128:1485–1495
21. **Robert P** 1995 Contribution a l'étude des domaines d'interaction entre les hormones gonadotropes hypophysaires et leurs récepteurs pharmacie. Paris: Université René Descartes de Paris; 101
22. **Bidart J, Troalen F, Bousfield GR, Birken S, Bellet DH** 1988 Antigenic determinants on human choriogonadotropin α-subunit. I. Characterization of topographic sites recognized by monoclonal antibodies. J Biol Chem 263: 10364–10369
23. **Bidart J-M, Troalen F, Bousfield GR, Bohuon C, Bellet D** 1989 Monoclonal antibodies directed to human and equine chorionic gonadotropins as probes

for the topographic analysis of epitopes on the human α-subunit. Endocrinology 124:923–929
24. **Matteri RI, Roser JF, Baldwin DM, Lipovetsky V, Papkoff H** 1987 Characterization of a monoclonal antibody which detects luteinizing hormone from diverse mammalian species. Dom Anim Endocrinol 4:157–165
25. **Butnev VY, Gotschall RR, Baker VL, Bousfield GR,** Influence of asparagine-56 oligosaccharide on in vitro subunit association and FSH receptor binding of equine gonadotropins. Proc of the 10th Int Congr of Endocrinol. 1996; abstract Pl-318
26. **Fox KM, Dias JA, Van Roey P** 2001 Three-dimensional structure of human follicle-stimulating hormone. Mol Endocrinol 15:378–389
27. **Maurel MC, Ban E, Bidart J-M, Combarnous Y** 1992 Immunochemical study of equine chorionic gonadotropin (eCG/PMSG): antigenic determinants on α- and β-subunits. Biochim Biophys Acta 1159:74–80
28. **Couture L, Lemonnier JP, Troalen F, et al.** 1993 Immunochemical studies of equine chorionic gonadotropin (eCG), eCG-α and eCG-β. Endocrinology 132: 205–211
29. **Butnev VY, Gotschall RR, Baker VL, Moore WT, Bousfield GR** 1996 Negative influence of *O*-linked oligosaccharides of high molecular weight equine chorionic gonadotropin on its luteinizing hormone and follicle-stimulating hormone receptor-binding activities. Endocrinology 137:2530–2542
30. **Hartree AS** 1975 Purification of human pituitary glycoprotein hormones. Methods Enzymol 37:380–389
31. **Hiyama J, Surus A, Renwick AGC** 1990 Purification of human pituitary LH and thyrotropin by hydrophobic chromatography. J Endocrinol 125:493–500
32. **Timossi CM, Barrios de Tomasi J, Zambrano E, Gonzalez R, Ulloa-Aguirre A** 1998 A naturally occurring basically charge human follicle-stimulating hormone (FSH) variant inhibits FSH-induced androgen aromatization and tissue-type plasminogen activator enzyme activity in vitro. Neuroendocrinology 67:153–163
33. **Laemmli UK** 1970 Cleavage of structural proteins during the assembly of the head of bacteriophage T4. Nature 227:680–685
34. **Hillenkamp F, Karas M, Beavis RC, Chait BT** 1991 Matrix-assisted laser desorption/ionization mass spectrometry of biopolymers. Anal Chem 63: 1193A–1203A
35. **Beavis RC, Chait BT** 1992 α-Cyano-4 hydroxycinnamic acid as a matrix for matrix-assisted laser desorption mass spectrometry. Org Mass Spectrom 27: 156–158
36. **von Heijne G** 1986 A new method for predicting signal sequence cleavage sites. Nucleic Acids Res 14:4683–4690
37. **Ozturk M, Bellet D, Manl L, Hennen G, Frydman R, Wands J** 1987 Physiological studies of human chorionic gonadotropin (hCG), αhCG, and βhCG as measured by specific monoclonal immunoradiometric assays. Endocrinology 120:549–558
38. **DeLean A, Munson PJ, Rodbard D** 1978 Simultaneous analysis of families of sigmoidal curves: application to bioassay, radioligand assay, and physiological dose-response curves. Am J Physiol 235:E97–E102
39. **Liu W-K, Bousfield GR, Moore Jr WT, Ward DN** 1985 Priming procedure and hormone preparations influence rat granulosa cell response. Endocrinology 116:1454–1459
40. **Korenman SG, Stevens RH, Carpenter LA, Robb M, Niswender GD, Sherman BM** 1974 Estradiol radioimmunoassay without chromatography: procedure, validation and normal values. J Clin Endocrinol Metab 38:718–720
41. **Wilkins MR, Williams KL** 1997 Cross-species identification using amino acid composition: a theoretical evaluation. J Theor Biol 186:7–15
42. **Shome B, Parlow AF, Liu WK, Nahm HS, Wen T, Ward DN** 1988 A reevaluation of the amino acid sequence of human follitropin β-subunit. J Protein Chem 7:325–339
43. **Sugino H, Takio K, Ward DN** 1989 Reevaluation of the amino acid sequence of porcine follitropin. J Protein Chem 8:197–219
44. **Bousfield GR, Butnev VY, Gotschall RR, Baker VL, Moore WT** 1996 Structural features of mammalian gonadotropins. Mol Cell Endocrinol 125:3–19
45. **Ward DN, Bousfield GR, Gordon WL, Sugino H** 1989 Chemistry of the peptide components of glycoprotein hormones. In: Keel BA, Grotjan Jr HE, eds. Microheterogeneity of glycoprotein hormones. Boca Raton: CRC Press; 1–21
46. **Dias JA, Lindau-Shepard B, Hauer C, Auger I** 1998 Human follicle-stimulating hormone structure-activity relationships. Biol Reprod 58:1331–1336
47. **Gordon WL, Bousfield GR, Ward DN** 1989 Comparative binding of FSH to chicken and rat testis. J Endocrinol Invest 12:383–392
48. **Chappel S, Zabrecky J, Hyman L, Nugent N, Gordon K, Bernstine E,** Characterization of bovine luteinizing hormone (bLH) produced by recombinant DNA technology. Proceedings of the 68th Annual Meeting of The Endocrine Society, Anaheim, CA 1986; abstract 610
49. **Parlow AF, Shome B** 1974 Specific, homologous radioimmunoassay (RIA) of highly purified subunits of human pituitary follicle stimulating hormone (hFSH). J Clin Endocrinol Metab 39:195–198
50. **Reichert Jr LE, Ward DN** 1974 On the isolation and characterization of the α- and β-subunits of human follicle-stimulating hormone. Endocrinology 94:655–664
51. **Rathnam P, Saxena BB** 1975 Primary amino acid sequence of follicle-stimulating hormone from human pituitary glands. I. α Subunit. J Biol Chem 250: 6735–6746
52. **Closset J, Hennen G** 1978 Porcine follitropin: isolation and characterization of the native hormone and its α and β subunits. Eur J Biochem 86:105–113
53. **Sairam MR** 1979 Studies on pituitary follitropin. II. Isolation and characterization of the subunits of the ovine hormone. Arch Biochem Biophys 194:71–78
54. **Parsons TF, Strickland TW, Pierce JG** 1984 Rapid and easy separation of the subunits of bovine and human glycoprotein hormones by use of high performance liquid chromatography. Endocrinology 114:2223–2227
55. **Bishop LA, Robertson DM, Cahir N, Schofield PR** 1994 Specific roles for the asparagine-linked carbohydrate residues of recombinant human follicle stimulating hormone in receptor binding and signal transduction. J Mol Endocrinol 8:722–731
56. **Stanton PG, Burgon PG, Hearn MTW, Robertson DM** 1996 Structural and functional characterization of hFSH and hLH isoforms. Mol Cell Endocrinol 125:133–141
57. **Wide L** 1986 The regulation of metabolic clearance rate of human FSH in mice by variation of the molecular structure of the hormone. Acta Endocrinol 112:336–344
58. **Green ED, Baenziger JU** 1988 Asparagine-linked oligosaccharides on lutropin, follitropin, and thyrotropin II. distributions of sulfated and sialylated oligosaccharides on bovine, ovine, and human pituitary glycoprotein hormones. J Biol Chem 263:36–44
59. **Lefort GP, Stolk JM, Nisula BC** 1984 Evidence that desialylation and uptake by hepatic receptors for galactose-terminated glycoproteins are immaterial to the metabolism of human choriogonadotropin in the rat. Endocrinology 115: 1551–1557
60. **Maack T, Park CH, Camargo MJF** 1992 Renal filtration, transport, and metabolism of proteins. In: Seldin DW, Giebisch G, eds. The kidney: physiology and pathophysiology, 2nd Ed. New York: Raven Press; 3005–3038
61. **Wu H, Lustbader JW, Liu Y, Canfield RE, Hendrickson WA** 1994 Structure of human chorionic gonadotropin at 2.6 Å resolution from MAD analysis of the selenomethionyl protein. Structure 2:545–558
62. **Lapthorn AJ, Harris DC, Littlejohn A, et al.** 1994 Crystal structure of human chorionic gonadotropin. Nature 369:455–461
63. **Rudd PM, Wormald MR, Stanfield RL, et al.** 1999 Roles for glycosylation of cell surface receptors involved in cellular immune recognition. J Mol Biol 293:351–366
64. **Sebok K, Sairam MR, Cantin M, Mohapatra SK** 1987 Distribution of follitropin and deglycosylated follitropin in the rat: a quantitative radioautographic study. Mol Cell Endocrinol 52:185–197
65. **Yding Andersen C, Leonardsen L, Ulloa-Aquirre A, Barrios-de-Tomasi J, Moore L, Byskov AG** 1999 FSH-induced resumption of meiosis in mouse oocytes: effect of different isoforms. Mol Hum Reprod 5:726–731